UDE-Based Robust Voltage Control of DC-DC Power Converters

Alon Kuperman
Hybrid Energy Sources R&D Laboratory
Ariel University
Ariel 40700, Israel
alonku@ariel.ac.il

***Abstract*—A method of linear robust controller design based on Uncertainty and Disturbance Estimator theory is proposed in the paper for nonlinear uncertain single input single output systems with external disturbances and applied to output voltage control of a unidirectional universal buck-boost converter. The controller forces the system to maintain nearly nominal performance through the whole range of operation space by quickly estimating and canceling the uncertainties and external disturbances. Despite the non-triviality and relative complexity of the method, the resulting controller structure is simple, allowing low cost low part count analog implementation. Extended simulation results are presented to demonstrate the effectiveness of the proposed method.**

***Keywords*—Uncertainty and disturbance estimator, Universal buck-boost dc-dc converter, Robust control**

I. INTRODUCTION

Battery powered systems have grown tremendously in recent decade. To prolong the service time of such devices, efficient power management circuits are required to extend the battery life. Consider e.g. a system with a 3.3 V power supply fed by a Li-Ion battery. During the discharge process, battery terminal voltage may drop from 4.2 to 2.5 V. In order to efficiently utilize the battery capacity a buck–boost dc–dc converter is the most appropriate choice. A non-inverting unidirectional converter, capable of operating in buck, boost and buck-boost modes has demonstrated remarkable performance, operating with battery-powered systems [1-6]. Despite impressive performance, such converter is not straightforward to modulate and control. Leaving aside modulation methods, since such a converter may operate in any of the three mentioned modes, three different transfer functions need to be treated by the controller. In addition, since the converter possesses nonlinear behavior, the transfer functions obtained by appropriate linearization are operating point dependent. In order to decrease the control design complexity, cascaded control structure is usually employed. Typical cascaded control structure of a power converter is shown in Fig. 1. The controller consists of two loops, usually decoupled in frequency domain. The outer (slow) loop performs output voltage regulation by comparing the sensed output voltage to a reference value, processing the difference to obtain a reference current for the inner (fast) inductor current loop. The latter creates a duty cycle signal by processing the difference between the reference and sensed inductor currents, acting as the control input to the power converter. The converter is fed by one controlled (duty cycle) and two uncontrolled (input voltage and load current) inputs. Decoupling of the voltage and current controllers allows each controller to interact with a first order plant and reject only one of the two disturbances. Moreover, while shaping one loop, the other one may be assumed "transparent", i.e. when the voltage controller is under consideration, the current loop may be treated as unity gain; when the current loop is concerned, voltage loop signals may be assumed constant.

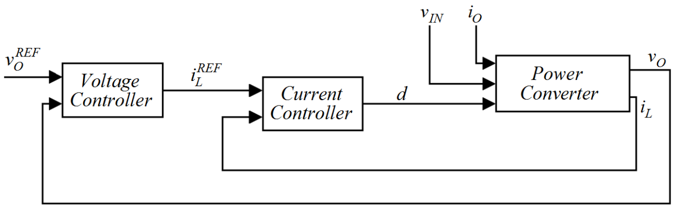

Fig. 1. Typical cascaded control structure of a power converter

Current controllers of power supplies are typically implemented by means of analog current-mode controllers, possessing extremely high bandwidths while completely rejecting input voltage disturbances (which are typically relatively slow). On the other hand, voltage controllers are more difficult to design since corresponding plants are nonlinear and the load current (disturbance) may vary significantly and with high rate. As a result, in case of analog implementation, voltage controller design is performed for a worst case, sacrificing the performance in other operating points. This drawback may be eliminated by a digital implementation at the expense of increased cost and complexity. In this paper, robust controller design is proposed allowing both analog implementation and maintaining nearly nominal performance through the whole operating region of the power converter.

The Uncertainty and Disturbance Estimator (UDE) based strategy introduced in [7] and further elaborated in [8], [9] is able to quickly estimate uncertainties and disturbances and thus provides excellent robust performance. It is based on the assumption that a continuous signal can be approximated as it is appropriately filtered. Recently, the two-degree of freedom nature of UDE controllers has been revealed in [10], which considerably facilitates the design of the controller. In this paper, the UDE-based control strategy is applied to solving the voltage control problem by stabilization, allowing the utilization of a single robust controller for all three converter modes of operation, achieving similar performance through the whole operating region.

II. LINEAR UDE-BASED CONTROL FOR NONLINEAR SISO SYSTEMS

Consider a nonlinear SISO system with uncertainties and disturbances described as

$$\begin{aligned}\dot{x}(t) &= g(x(t),t) + b(x(t),t)u(t) + f(x(t),u(t),d(t),t) \\ y(t) &= x(t) + n(t)\end{aligned} \quad . \tag{1}$$

Here x is the state, u the control input, d the unknown disturbance, g the known smooth nonlinear function of the state, f the unknown smooth nonlinear function of the state, control input and unknown disturbance, n is the measurement noise and $b = B_1+B_2(x,t)$ is a control function of the state, where B_1 is a nonzero constant and B_2 a function of the state.

A linear time invariant reference model is chosen according to the desired state behavior as

$$\dot{x}_m(t) = A_m x_m(t) + B_m c(t) \tag{2}$$

and the control objective is to force a stable error between the state of the reference model and the state of the system,

$$e(t) = x_m(t) - x(t) \tag{3}$$

and satisfy the error dynamic equation

$$\dot{e}(t) = \left(A_m + K\right)e(t) \; . \tag{4}$$

Here, K is an error feedback gain, x_m is the reference state vector and c is a piecewise continuous and uniformly bounded reference signal (in order to simplify the exposition, the arguments of functions in the time-domain are omitted hereafter). If the reference model is chosen to be stable, K may be chosen as zero. If different error dynamics is desired or required to guarantee stability, commonly used control strategies can be used to choose K.
Combining equations (1) – (4) results in

$$A_m x + B_m c - g - bu - f = Ke \, , \tag{5}$$

hence the control signal u needs to satisfy

$$bu = A_m x + B_m c - Ke - g - f \; . \tag{6}$$

Denote the terms that include the uncertainties, the external disturbance and the nonlinear dynamics in (6) as $h \triangleq -g - f - B_2 u = -\dot{x} + B_1 u$, bringing the system (1) to the following form,

$$\dot{x} = B_1 u - h \; . \tag{7}$$

The function h is referred to as total uncertainty and disturbance (TUD). Hence, the unknown/nonlinear dynamics and disturbances can be obtained from the known linear dynamics of the system and the control signal. However, it cannot be directly used to formulate a control law. The UDE-based strategy proposed in [20] adopts an estimation of the TUD to construct a control law. Assume that $g_f(t)$ is the impulse response of a linear filter $G_f(s)$, whose pass-band contains the frequency content of h. Then TUD can be accurately estimated from the output of the UDE as

$$h_{ude} = h * g_f \, , \tag{8}$$

where '*' is the convolution operator. Substituting (8) back into (6) instead of TUD re-defines the control signal requirements as

$$B_1 u = A_m x + B_m c - Ke - h_{ude} = A_m x + B_m c - Ke - \left(\dot{x} - B_1 u\right) * g_f \, . \tag{9}$$

Applying the Laplace transform and rearranging, following desired control law is obtained,

$$U(s) = \frac{B_1^{-1}}{1 - G_f(s)}\left[A_m X(s) + B_m C(s) - KE(s) - sX(s)G_f(s)\right] \tag{10}$$

Obviously, the control signal has nothing to do with the unknown dynamics and disturbances. Note that when $G_f(s)$ is strictly proper, $sG_f(s)$ is implementable and there is no need of measuring or estimating the derivative of the state. Since measured state fed back to the controller is corrupted by additive noise (see the output equation in (1)); substituting $X(s)$ with $Y(s)$ in (10) makes the actual control signal to contain noise as well,

$$\begin{aligned}U(s) &= \frac{B_1^{-1}}{1 - G_f(s)}\left[A_m Y(s) + B_m C(s) - KE(s) - sG_f(s)Y(s)\right] \\ &= \frac{B_1^{-1}}{1 - G_f}\left[A_m X + B_m C - KE - sG_f X + A_m N - sG_f N\right]\end{aligned} \tag{11}$$

Substituting (11) into (1) and taking into account the Laplace transform of (2), the closed loop state dynamics is obtained as

$$X(s) = Z_m(s)C(s) + Z_1(s)\left(Z_2(s)H(s) + Z_3(s)N(s)\right) , \tag{12}$$

where $Z_m(s) = (s - A_m)^{-1}B_m$ is the reference model transfer function, $Z_1(s) = -(s - [A_m+K])^{-1}$, $Z_2(s) = 1 - G_f(s)$ and $Z_3(s) = A_m - sG_f(s)$. Note that $Z_m(s)$ is independent on K and G_f, therefore the proposed control law allows decoupling between tracking (determined by $Z_m(s)$) and noise/disturbance rejection (governed by $Z_1(s)$, $Z_2(s)$ and $Z_3(s)$).

The resulting error dynamics is obtained by combining (1), (2), (3) and (11) as

$$E(s)=Z_1(s)\left(Z_2(s)H(s)+Z_3(s)N(s)\right)\ . \tag{13}$$

According to (13), TDU is attenuated twice: first by a low-pass filter Z_1(s); second by the filter $Z_2(s)$, possessing high-pass filter properties if $G_f(s)$ is strictly proper. Measurement noise is shaped twice as well, initially by the low-pass filter $Z_1(s)$ and then by a frequency selective filter $Z_3(s)$. In order to assure that the actual system (1) follows the reference model (2), the right-hand side of (13) must be close to zero in steady state. This is satisfied if $Z_1(s)\cdot Z_2(s)$ and $Z_1(s)\cdot Z_3(s)$ are close to zero at the frequency range where $H(s)$ and $N(s)$, respectively, possess significant energy. Note that $Z_1(s)$ independent on G_f, and is decoupled from $Z_2(s)$ and $Z_3(s)$, allowing separate design of the filter $Z_1(s)$ by selecting appropriate K. On the other side, filters $Z_2(s)$ and $Z_3(s)$ are related since both depend on G_f while A_m is forced by the reference model.

Keeping in mind that the controller should be as simple as possible to allow low part count analog implementation, consider the first order Butterworth filter, given by

$$G_f(s)=\frac{1}{Ts+1}\ , \tag{14}$$

leading to $Z_2(s)=\dfrac{Ts}{Ts+1}$ and $Z_3(s)=A_m\dfrac{\left(T-A_m^{-1}\right)s+1}{Ts+1}$. Obviously, $Z_2(s)$ is a high pass filter and $Z_3(s)$ is a lead-lag filter. Moreover, remarking that stable reference model requires negative A_m with $|A_m|=|B_m|$ and noting that $\dfrac{1}{1-G_f}=1+\dfrac{1}{Ts}$ and $\dfrac{sG_f}{1-G_f}=\dfrac{1}{T}$, the control action in (11) reduces to

$$U=B_1^{-1}\left(\left[1+\frac{1}{Ts}\right]\left[B_m\left(C-Y\right)-KE\right]-\frac{1}{T}Y\right). \tag{15}$$

Block diagram of the corresponding control structure is shown in Fig. 2.

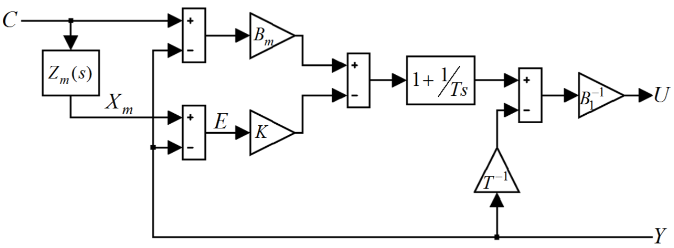

Fig. 2. UDE-based controller block diagram

In case the reference signal $c(t)$ is constant, tracking dynamics has no meaning (assuming that during start-up the initial transients are governed by a soft-start sequence) and the disturbance rejection is the main issue. In order to robustify the system against TUD, the corner frequency of $Z_1(s)$ should be as low as possible, while the corner frequency of $Z_2(s)$ should be as high as possible. As to measurement noise (which usually resides at the high frequency portion of the spectrum), the requirement regarding the corner frequency of $Z_1(s)$ is the same. As to $Z_3(s)$, for $|A_m|>1$ it amplifies the high frequency noise. As a result, if the reference model may be chosen relatively slow, the corner frequency of $Z_1(s)$ will be reduced as well as the high frequency gain of $Z_3(s)$. Moreover, for low enough $|A_m|$ the gain K may be selected as zero, simplifying the controller and reducing the parts count.

III. Application to Current-Controlled DC-DC Converters

Consider a universal non-inverting unidirectional dc-dc converter, shown in Fig. 3. The circuit may operate in any of the three modes: buck (T_2 is constantly off, T_1 is switched), boost (T_1 is constantly on, T_2 is switched) and buck-boost (T_1 and T_2 are simultaneously switched).

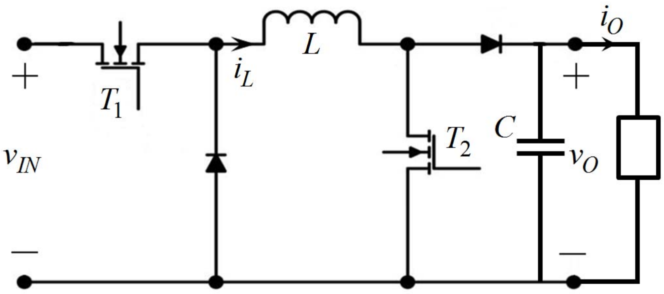

Fig. 3. Universal noninverting unidirectional dc-dc converter

An idealized average model of the converter is shown in Fig. 4. In buck mode, T_1 duty cycle is $d_1=d$ and T_2 duty cycle is $d_2=0$. In boost mode, T_1 duty cycle is $d_1=1$ and T_2 duty cycle is $d_2=d$. In buck-boost mode, T_1 and T_2 duty cycles are equal, $d_1=d_2=d$.

The average model is described by the following sets of equations, depending on the mode of operation:

$$\left.\begin{aligned}\frac{di_L}{dt}&=\frac{1}{L}\left(dv_{IN}-v_O\right)\\ \frac{dv_O}{dt}&=\frac{1}{C}\left(i_L-i_O\right)\end{aligned}\right\}buck\ , \tag{16}$$

$$\left.\begin{aligned}\frac{di_L}{dt}&=\frac{1}{L}\left(v_{IN}-(1-d)v_O\right)\\ \frac{dv_O}{dt}&=\frac{1}{C}\left((1-d)i_L-i_O\right)\end{aligned}\right\}boost\ , \tag{17}$$

$$\left.\begin{aligned}\frac{di_L}{dt}&=\frac{1}{L}\left(dv_{IN}-(1-d)v_O\right)\\ \frac{dv_O}{dt}&=\frac{1}{C}\left((1-d)i_L-i_O\right)\end{aligned}\right\}buck-boost\ . \tag{18}$$

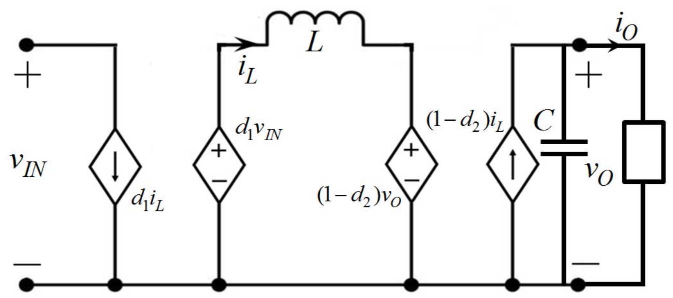

Fig. 4. Average model of the converter

If the current loop is properly closed, the inductor current may be assumed to perfectly follow its reference when designing the voltage controller, i.e. $i_L = i_L^*$. As a result, the plant to be regulated by the voltage controller is given by

$$\dot{v}_O = C^{-1}\left(i_L^* - i_O\right),\ buck\,, \tag{19}$$

$$\dot{v}_O = C^{-1}\left((v_{IN} - L\frac{di_L^*}{dt})v_O^{-1} i_L^* - i_O\right),\ boost\,, \tag{20}$$

$$\dot{v}_O = C^{-1}\left((v_{IN} - L\frac{di_L^*}{dt})(v_{IN} + v_O)^{-1}) i_L^* - i_O\right),\ buck-boost\,, \tag{21}$$

respectively, for each operation mode. Note that the capacitance does not remain constant during the operation and may be denoted as a sum of nominal and varying parts, $C^{-1} = C_n^{-1} + \Delta C^{-1}(t)$. Moreover, note that un-modeled dynamics is present since passive components and conducting MOSFETS possess equivalent series resistances (ESR) and diodes forward voltages (V_F) are nonzero. Consequently, the three plants are nonlinear in practice (even though the idealized plant is linear in buck mode). A general plant, describing (19)-(21) is given by

$$\dot{v}_O = C_n^{-1} i_L^* - h\,, \tag{22}$$

where the TUD function h is different in each operation mode. Note that (22) is of the same structure as (7) and hence may be controlled similarly. The control problem is to regulate the output voltage to a constant value. Since there will be no reference signal changes, tracking dynamics may be sacrificed and as a result K is set to zero in (15). The resulting controller is given by

$$U(s) = C_n\left(B_m\left[1 + \frac{1}{Ts}\right]\left(V_O^{REF}(s) - V_O^s(s)\right) - \frac{1}{T}V_O^s(s)\right), \tag{23}$$

where V_O^{REF} is the output voltage reference and V_O^s is the sensed output voltage. Obviously, the control design is reduced to selecting B_m and T only.

IV. Example

Consider a battery powered system, based on the non-inverting, unidirectional buck-boost universal dc-dc converter, shown in Fig. 3. The converter is feeding a dynamic load and is supplied by a Li-Ion battery pack of 4 series connected cells. As a result, the input voltage of the converter may vary from 4·4.2 = 16.8 V (full pack) down to 4·2.5 = 10 V (empty pack) while the load voltage is required to be regulated to a constant level of 13 V. The system is designed such that the converter operates in buck mode when the input voltage is higher than 13 V, passing to buck-boost mode when the input voltage is around 13 V and ends up in boost mode when the input voltage reduces below 13 V. Assume that the current loop operates properly with high bandwidth. The values of converter components along with the values of parasitic elements are given in Table I. Note that neither of the parameters is known to the controller.

TABLE I
Converter components values

Parameter	Value	Units
Inductance L	1	mH
ESR(L)	5	mΩ
Capacitance C	940	μF
ESR(C)	1	mΩ
ESR(T_1)	20	mΩ
ESR(T_2)	20	mΩ
$V_F(D_1)$	0.5	V
$V_F(D_2)$	0.5	V

The reference model dynamics was selected as B_m = 20π and the UDE filter time constant was chosen as $T = (20000\pi)^{-1}$. Nominal capacitance C_n was set to 500 μF. The consequent bode diagrams of Z_m and Z_1-Z_3 are shown in Fig. 5, where the frequency characteristics, mentioned earlier are evident.

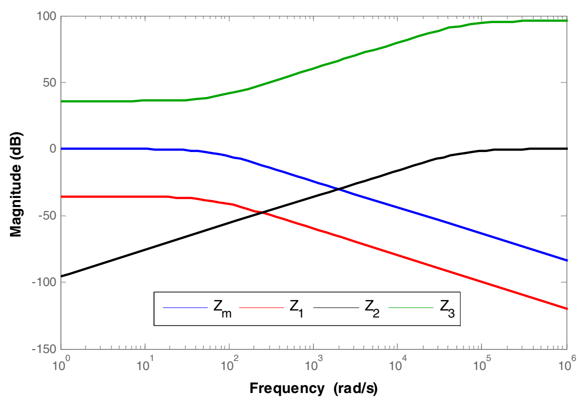

Fig. 5. Frequency responses of filters Z_m and Z_1-Z_3

Frequency responses of TUD and noise shaping filters $Z_{12}(s) = Z_1(s)\cdot Z_2(s)$ and $Z_{13}(s) = Z_1(s)\cdot Z_3(s)$ are shown in Figs. 6 and 7, respectively. Obviously, the TUD is processed by a band-pass filter with worth case attenuation of around -95 dB while the noise is shaped by a low-pass filter with corner frequency of around 60 kHz. Hence, the converter switching frequency should be selected above this corner frequency in order to attenuate switching noise and was set to 100 kHz in the simulations.

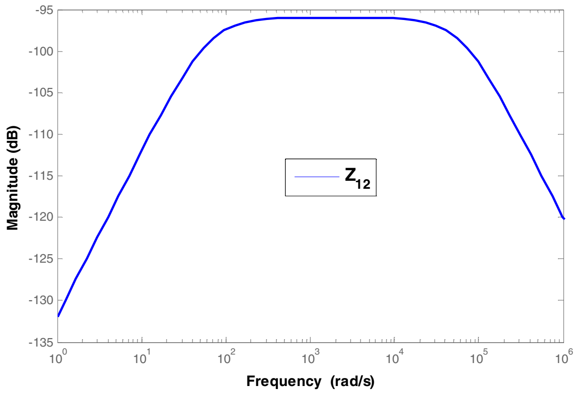

Fig. 6. Frequency response of TUD shaping filter Z_{12}

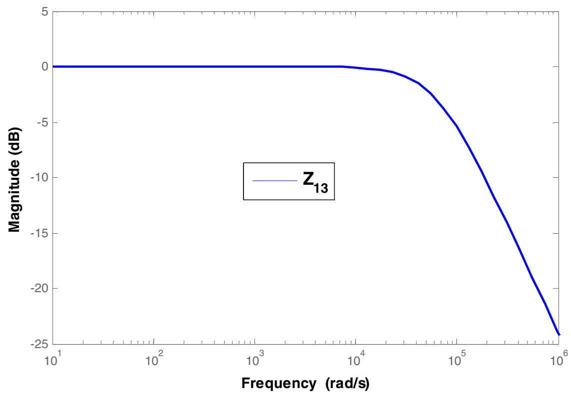

Fig. 7. Frequency response of noise shaping filter Z_{13}

The system was simulated using PSIM software. Simulation circuit is shown in Fig. 8. The battery pack is modeled using a variable voltage source while the consists of passive and active components. A 13 Ω resistor represents the constant component while pulsed current load of 2 A peak-to-peak plays the role of the dynamic component. Voltage controller is implemented according to (23) and drives the current controller and modulator.

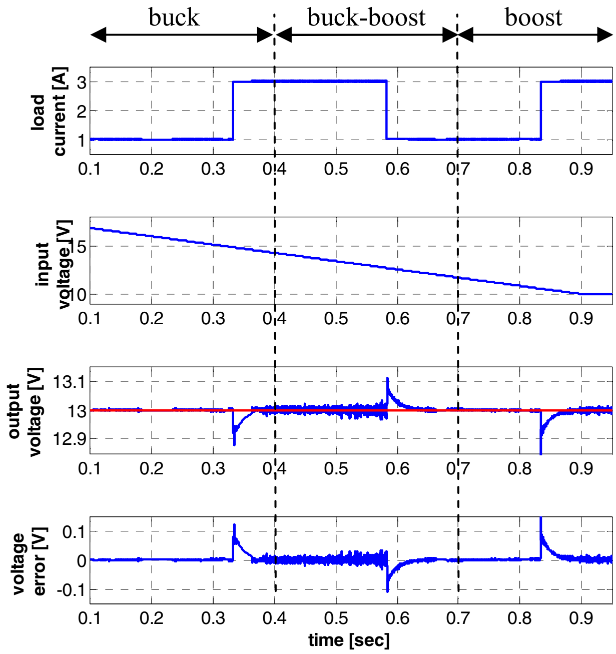

Fig. 9. Simulation results (from top to bottom): Load current; Input voltage; Reference and output voltages; Voltage error.

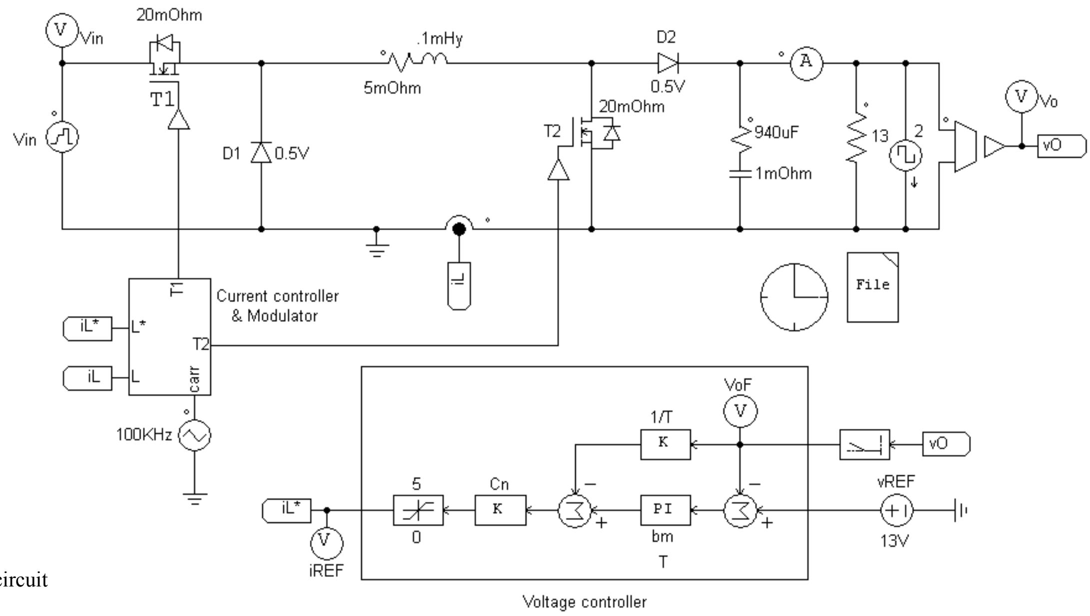

Fig. 8. Simulation circuit

Simulation results are shown in Fig. 9. The system operates with no steady-state error in all three modes of operation, quickly rejecting the uncertainties and disturbances.

V. CONCLUSIONS

A method of designing a linear robust controller for nonlinear uncertain single input single output systems with external disturbances, based on Uncertainty and Disturbance Estimator theory was proposed in the paper. The approach was successfully applied to control the output voltage of a unidirectional universal buck-boost converter. By quickly estimating and canceling the uncertainties and disturbances, the controller forces the system to maintain nearly nominal performance through the whole range of operating points. Despite the relatively non-trivial and complex underlying theory, the resulting controller structure turns out to be relatively simple, allowing low cost analog implementation with low part count. Extended simulation results were presented to demonstrate the feasibility of the proposed method.

REFERENCES

[1] B. Sahu and G. A. Rincon-Mora, "A low voltage, dynamic, noninverting, synchronous buck–boost converter for portable applications," *IEEE Trans. Power Electron*., vol. 19, no. 2, pp. 443–452, Mar. 2004.

[2] Y. H. Lee, S. C. Huang, S. W. Wang, W. C. Wu, P. C. Hung, H. H. Ho, Y. T. Lai, and K. H. Chen, "Power-tracking embedded buck–boost converter with fast dynamic voltage scaling for SoC system," *IEEE Trans. Power Electron*., vol. 27, no. 3, pp. 1270–1282, Mar. 2012.

[3] Y. J. Lee, A. Khaligh, and A. Emadi, "A compensation technique for smooth transitions in a noninverting buck–boost converter," *IEEE Trans. Power Electron*., vol. 24, no. 4, pp. 1002–1116, Apr. 2009.

[4] C. Restrepo, J. Calvente, A. Cid-Pastor, A. E. Aroudi, and R. Giral, "A non-inverting buck–boost dc–dc switching converter with high efficiency and wide bandwidth," *IEEE Trans. Power Electron*., vol. 26, no. 9, pp. 2490–2503, Sep. 2011.

[5] C. L. Wei, C. H. Chen, K. C. Wu and I. T. Ko, "Design of an average current mode noninverting buck-boost dc-dc converter with reduced switching and conduction losses," *IEEE Trans. Power Electron*., vol. 27, no. 12, pp. 4934–4942, Dec. 2012.

[6] A. Kuperman, I. Aharon, S. Malki and A. Kara, "Design of a semiactive battery-ultracapacitor hybrid energy source," *IEEE Trans. Power Electron*., vol. 28, no. 2, pp. 806–815, Feb. 2013.

[7] Q.-C. Zhong and D. Rees, "Control of uncertain LTI systems based on an uncertainty and disturbance estimator," *Jour. Dyn. Sys. Meas. Con. - Trans. ASME*, vol. 126, pp. 905-910, 2004.

[8] A. Kuperman and Q.-C. Zhong, "Robust control of uncertain nonlinear systems with state delays based on an uncertainty and disturbance estimator," *Int. Jour. Nonl. Robust Contr*, vol. 21, pp. 79 – 92, 2011.

[9] R. Stobart, A. Kuperman and Q.-C. Zhong, "Uncertainty and disturbance estimator (UDE) based control of uncertain linear systems with state-delays," *Jour. Dyn. Sys. Meas. Con. - Trans. ASME*, vol. 133, no. 2, pp. 1 – 6, 2011.

[10] Q.-C. Zhong, A. Kuperman and R. Stobart, "Design of UDE-based controllers from their two-degree-of-freedom nature," *Int. Jour. Nonl. Robust Contr.*, vol. 21, pp. 1994 – 2008, 2011.